JOURNAL OF GEOPHYSICAL RESEARCH, VOL. 85, NO. C3, PAGES 1524–1530, MARCH 20, 1980

Local and Shoaled Comparisons of Sea Surface Elevations, Pressures, and Velocities

R. T. GUZA

Shore Processes Laboratory, Scripps Institution of Oceanography, University of California La Jolla, California 92037

EDWARD B. THORNTON

Naval Postgraduate School, Monterey, California 93940

Sea surface elevations, or pressures, and velocities were measured at closely spaced (wavelength or less) locations in a line extending from 10-m depth to inside the surf zone at Torrey Pines Beach, San Diego, California. Intercomparisons of local pressure, velocity, and sea surface elevation spectra for the wind wave frequencies (0.05–0.3 Hz) were made by using linear wave theory. Errors in both total variance and energy density in a particular frequency band are less than 20% both inside and outside the surf zone, except in the immediate vicinity of the breakpoint, where larger disparities are observed. Surface elevation spectra calculated at 10 m were shoaled by using linear wave theory. The total variance of stations between 10- and 3-m depth are typically predicted with less than 20% error, although harmonic amplification and other nonlinear effects can lead to significant errors in the prediction at particular frequency bands. Observations inside 3-m depth significantly departed from the predictions of linear shoaling theory.

INTRODUCTION

Models for the fluid and sediment dynamics of the surf zone and inner shelf usually make the assumption that linear wave theories provide an acceptable lowest-order description of the wave dynamics. Specifically, it is commonly assumed that outside the surf zone, changes in the wave field during propagation toward the beach are governed by Snell's law and conservation of energy. Relationships between the local sea surface elevation and velocity (or pressure) field at depth are generally assumed to be given by flat bottom linear Airy theory both inside and outside the surf zone [e.g., *Bowen*, 1969; *Longuet-Higgins*, 1970; *Komar and Inman*, 1970]. Considering the widespread application of these assumptions, there have been surprisingly few field experiments to test them.

Comparisons between spectra of sea surface elevation (or pressure) and velocity, measured at the same horizontal location in relatively shallow water, have been made by various authors. *Bowden and White* [1966] and *Simpson* [1969] made observations in 4- to 6-m depth, and the spectral peaks were about 0.2 Hz, yielding $0.7 < h/L < 0.1$, with h the mean water depth and L the deepwater wavelength of the spectral energy peak. *Thornton and Krapohl* [1974] studied long Pacific swell (0.06 Hz) in 19-m depth, $h/L = 0.04$. *Cavaleri et al.* [1978] took data in 16-m depth, with peak spectral energy at 0.2 Hz, yielding $h/L = 0.4$. In these cases the Ursell number $Ur = a/h(kh)^2$ (with the amplitude a taken as $a_{1/3} = H_s/2 = 2v$, with v^2 the total variance, and k as the wave number of the spectral peak) was less than 0.09. Limits on the validity of Stokes-type gravity wave theory (linear Airy waves being the lowest-order solution) for long waves are usually set around $Ur < 0.3$ [e.g., *Madsen*, 1971]. These measurements are therefore of weakly nonlinear waves, at a distance many surf zone widths offshore, and in depths where Airy theory can be expected to be reasonably accurate. Measured horizontal velocity spectra generally agree with predicted spectra (using linear theory and pressure sensors or wave staffs at the same location as input) with about 10% error in the vicinity of the spectral peak, although Simpson's data showed a larger disagreement of about 30%. *Esteva and Harris* [1970] observed very good agreement between sea surface and pressure in 4.7-m depth, with Ursell numbers ranging up to 1.5, although similar measurements by *Homma et al.* [1966] showed factor of 2 disparities in variance between sea surface elevation and depth-compensated pressure.

In the present work, linear comparisons of pressure, sea surface, and velocity are made for both small and large Ursell numbers. The physical region covered is from 10-m depths ($Ur < 0.05$) to about 1-m depth ($Ur \gg 1$, $a/h = O(1)$) inside the surf zone. Clearly, nonlinear theory is required to describe fully the dynamics throughout this range, but there is presently no such theory for a spectrum of waves. Thus the present comparisons made between sea surface elevation η (or pressure P) and velocity u measured at the same location in the horizontal plane experimentally address the question of whether nonlinearities are locally strong enough to distort significantly the P, u, η relationships given by linear theory.

The effects of nonlinearities on the shoaling transformation is, of course, a cumulative one. Nonlinearities may be locally weak, but significant cross-spectral transfer can occur if the shoaling region is wide in comparison to a nonlinear interaction distance. It should be noted that the large interaction distances (hundreds of kilometers) associated with deepwater gravity wave cubic interactions will be vastly reduced in the shallow water shoaling region. It is known that the flat bottom, Korteweg-deVries (finite amplitude, shallow water) equations allow significant cross-spectral energy transfers due to nearly resonant quadratic interactions [*Mei and Ünlüata*, 1972]. It would be expected that on a sloping beach the rate of transfer would increase as the depth decreases, since the increasing Ursell number leads to shorter interaction distances. Very gentle slopes will favor cross-spectral transfers, since the waves traverse a long distance in shallow water. When significant cross-spectral energy transfers occur, the usual linear shoaling theory which predicts the variance of each frequency

Paper number 9C1668.
0148-0227/80/009C-1668$01.00

band, independently of other frequencies, will be inaccurate. It is not known, theoretically, how gentle beach slopes must be for significant nonlinear transfers to occur. There apparently have been no field studies where incident waves were measured at closely spaced (of the order of a dominant wavelength or less) intervals throughout the shoaling region on a topography simple (and well known) enough to allow testing of linear shoaling theory. Here field data from a gently sloping beach (1.3°) clearly show nonlinear shoaling effects but also demonstrate the ability of linear shoaling theory to predict qualitatively total wind wave variance (except near the breakpoint) given the spectra of incident waves in 10-m depth.

THEORY

Linear wave theory describes the local sea surface elevation $\eta(t)$ as the superposition of an infinite number of independent sinusoids

$$\eta(t) = \sum_{n=1}^{\infty} a_n \cos(k_n \cdot x + \sigma_n t + \epsilon_n) = \sum_{n=1}^{\infty} \eta_n \tag{1}$$

where a_n is the amplitude, x is the horizontal coordinate vector, t is the time, ϵ_n is the phase angle, k_n is a horizontal vector wave number, and σ_n is the frequency related in linear theory to k by

$$\sigma_n^2 = g|k_n| \tanh |k_n|h \tag{2}$$

where g is the acceleration of gravity and h is the total local water depth. The equations for the horizontal velocity and pressure are

$$u(t) = \sum_{n=1}^{\infty} \frac{a_n \sigma_n \cosh |k_n|(h+z)}{\sinh |k_n|h} \cos(k_n \cdot x + \sigma_n + \epsilon_n)$$

$$= \sum_{n=1}^{\infty} \left[\frac{\sigma_n \cosh |k_n|(h+z)}{\sinh |k_n|h}\right] \eta_n \tag{3}$$

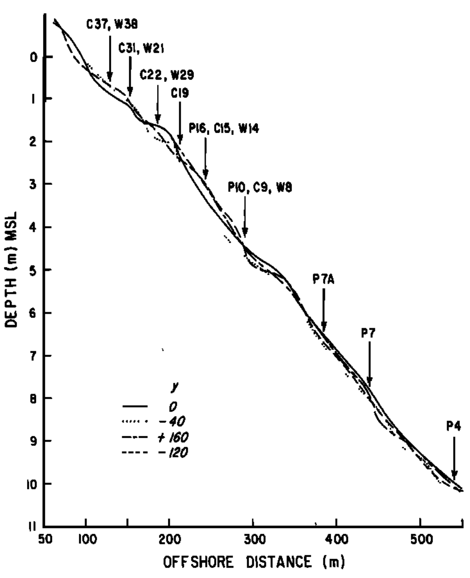

Fig. 1. Representative beach profiles, November 18. Sensors are located on the onshore-offshore range line with longshore coordinate $y = 0$. Offshore distances are from an arbitrary datum. Sensor types are identified as P for pressure, C for current, and W for surface-piercing staff.

TABLE 1. Heights of Sensing Elements Above the Seabed

Sensor	Depth Above Bed, cm
P4	35
P7	58
P7A	32
P10	36
C9	98
P16	55
C15	61
C19	89
C22	57
C37	46
C39	41

and

$$P(t) = -\rho g z + \sum_{n=1}^{\infty} \left[\frac{\cosh |k_n|(z+h)}{\cosh |k_n|h}\right] \rho g \eta_n \tag{4}$$

respectively, where z is the depth of interest measured positively upward from still water level. The bracketed terms in (3) and (4) are the spectral transfer functions relating velocity and pressure spectra to elevation spectra.

In water of slowly varying depth the wave amplitudes and wave numbers are also slowly varying functions. Equation (2) gives the magnitude of the wave numbers, while the direction is obtained by application of Snell's law. The amplitude variation is based on the theory of wave intensity along a refracted ray [*Munk and Arthur,* 1952]. These are statements of the usual linear wave refraction techniques in the absence of mean currents and reflection [*Dobson,* 1967].

MEASUREMENTS

Experiments were conducted at Torrey Pines Beach, San Diego, California, during November 1978. This is a gently sloping, moderately sorted, fine-grained (mean diameter 0.1 mm) sandy beach. An extensive array of instruments was deployed to study nearshore wave dynamics. The locations of instruments used in this study in relation to onshore-offshore profiles are shown in Figure 1.

The pressure sensors were Stathem temperature-compensated transducers with dynamic range of either 912–2316 g/cm^2 or 912–3720 g/cm^2. Output stage amplifiers were used to increase resolution. All pressure sensors were statically precalibrated and postcalibrated by being lowered into a saltwater tank and are quite linear. Precalibrated and postcalibrated gains differed by less than 2%.

Current meters were two-axis, Marsh-McBirney electromagnetic, spherical (4-cm diameter) probes with a three-pole output filter at 4 Hz. Under dc flows this probe is known to have a gain change around 80 cm/s [e.g., *Lavelle et al.,* 1978] associated with transition of the boundary layer on the probe head. Similar detailed results for broadband oscillatory flows are not available. Preliminary experiments [*Cunningham et al.,* 1979], with both sinusoidal and pseudorandom noise velocity fields indicate that the probe has hydrodynamic properties which make the gain at any particular frequency a weak function of the entire velocity field. Precalibration and postcalibration of current meters showed little change, in replicate runs, with steady or oscillating velocity fields. Thus in current meter calibration the problem is not variation of gain during the period of the installation but an uncertainty about the dynamic response of the instrument. Although the gains observed in calibration runs vary slightly with the amplitude of an imposed sinusoidal velocity field, implying nonlinear effects, spurious current signals at harmonics of the imposed motion are less than one-thirtieth the primary amplitude ($<10^{-4}$ in power). The gains used in processing these data are the values obtained by towing the instrument at 100 cm/s through still fluid.

It is possible that the observed gain differences reflect errors in the calibration procedure and apparatus rather than problems in probe response. Nevertheless, lacking more definitive calibration of the current meters, the present calibration runs must be used. On the basis of these tests the uncertainty associated with using a single gain factor for all frequencies is roughly estimated at ±5% in amplitudes (10% in variances).

The wave staffs are dual resistance wires with low noise, high resolution, and good electronic stability. Gain accuracy is about ±3%. Thus in comparisons of wave height (or pressure) to velocity signals the combined gain uncertainty is about 8%, limiting quantitative comparisons to this level. All instruments were mounted on pipes which had been fluidized into the sand bed. Current meters were oriented by using a bubble level and compass. Heights of sensing elements above the seabed are shown in Table 1, as measured on November 18, 1978, and are typical of all data runs.

Data were retrieved from the sensors by telemetering the data to shore, where it was recorded on a special receiver/tape recorder described in detail by *Lowe et al.* [1972]. The sampling rate was 64 samples/s, which was then low -pass- filtered and reduced to 2 samples/s.

LOCAL COMPARISONS

Velocity and pressure spectra measured at depth are related to sea surface elevation, using linear theory, through (3) and (4). Figure 2 shows a typical comparison outside the breakpoint where all sensors have been used to calculate sea surface elevation spectra. The spectral densities of the two orthogonal components of horizontal velocity measured by the current meter were summed, yielding the horizontal velocity spectral density (3). The agreement is good between 0.05 and 0.3 Hz, and much of the observed difference can be attributed to calibration inaccuracies. For higher frequencies, instrument noise is being amplified through the large correction to sea surface elevation. A significant wave height $H_s = 4\nu$ is used as a reference wave height, where ν^2 is the total variance between 0.05 and 0.3 Hz. In this particular example, $H_s^\eta = 100$ cm, $H_s^p = 97$ cm, and $H_s^u = 94$ cm, each H_s being derived from the calculated sea surface elevation spectrum. Of course, the measured sea surface elevation (or pressure) could be used to predict the velocity spectrum. Each spectral estimate for η in Figure 2 would be multiplied by the factor (equation (3)) $[\sigma_n \cosh k_n (h + z)/\sinh k_n h]^2$, and the basic agreement would be unaltered. The Ursell number based on H_s and the k of the spectral peak is 1.10, and $a_{sig}/h = 0.09$. In the present context, H_s should be viewed simply as a quantity proportional to the square root of the variance. The usual interpretation as a wave height statistic is rigorous only for Gaussian processes, and many of the time series considered here are distinctly non-Gaussian.

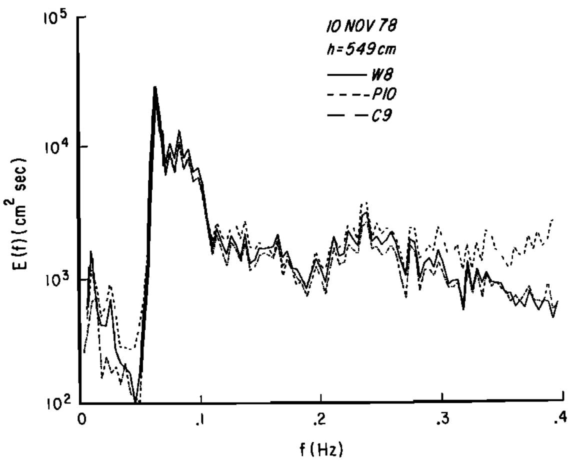

Fig. 2. Spectra of directly measured sea surface elevation (W8) and sea surface calculated (equations (3) and (4)) from pressure (P10) and horizontal velocity (C9) measured near the bottom. The data run is 102 min, and there are 48 degrees of freedom.

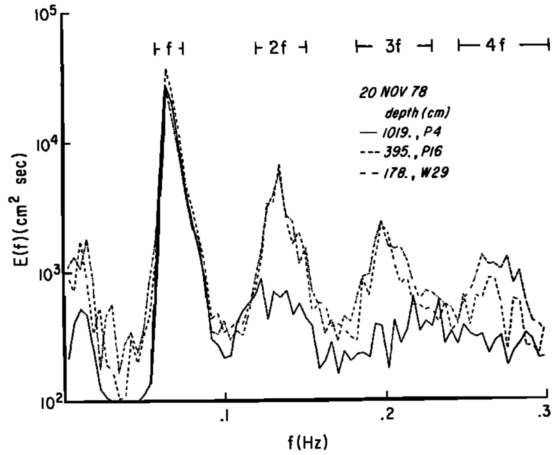

Fig. 3. Sea surface elevation spectra illustrating growth of harmonics during shoaling.

Uncertainties in the total depth introduce errors in the comparison of data to linear theory. It follows from (3) and (4) that for relatively long waves, H_s^p is insensitive to the total depth, since the pressure is almost hydrostatic. However, H_s^u has an error $\Delta h/2h$, where h and Δh are the total depth and depth uncertainty. Typically, Δh is at most 15 cm for surf zone sensors and 30 cm offshore, where surveying was infrequent. The resulting errors in H_s^u are generally less than 10%.

The increasing importance of nonlinearities in shallow water is illustrated in Figure 3. Energetic narrow band swell (0.065 Hz), with very low energy at higher frequencies, is observed in 10-m depth. In shallow depths the waves have become peaky with increased energy in the harmonics. Amplification of harmonics of the spectral peak may also be occurring in Figure 2, but it is submerged in the relatively high background level of incident high-frequency wind waves.

A qualitative idea of the importance of nonlinearity is given by the ratio $E(nf)/E(f)$, where $n = 2, 3, 4$ are the harmonic

TABLE 2. Ratio of Harmonic Energy to Primary Frequency Energy

	Depth, cm		
$E(nf)/E(f)$	1019	395	178
$E(2f)/E(f)$	0.08	0.32	0.39
$E(3f)/E(f)$	0.07	0.16	0.270
$E(4f)/E(f)$	0.06	0.072	0.20
a_s/h	0.04	0.11	0.25

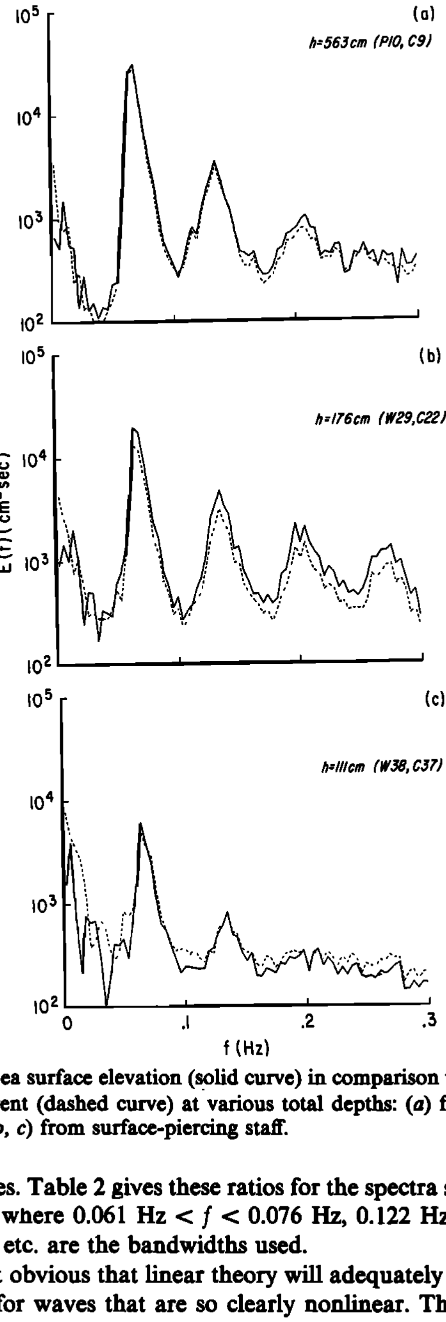

Fig. 4. Sea surface elevation (solid curve) in comparison with horizontal current (dashed curve) at various total depths: (*a*) from pressure and (*b, c*) from surface-piercing staff.

frequencies. Table 2 gives these ratios for the spectra shown in Figure 3, where 0.061 Hz $< f <$ 0.076 Hz, 0.122 Hz $< 2f <$ 0.152 Hz, etc. are the bandwidths used.

It is not obvious that linear theory will adequately relate P, u, and η for waves that are so clearly nonlinear. The Korteweg-deVries equations show that $O(a/h)$ errors arise in using linear theory to relate P, u, and η, and the size of this term can be significant, as is shown in Table 2. Thus significant errors might be expected to occur, particularly in relating the higher harmonics of P, u, and η to each other.

Surprisingly, the data show the local P, u, η agreement using linear theory to be rather good everywhere. Figure 4 shows comparisons of surface elevation predicted from horizontal velocity (E_u) to that calculated from pressure (E_p) or directly measured sea surface elevation (E_η) well outside the surf zone (h = 563 m), just outside the surf zone (h = 176 cm), and inside the surf zone (h = 111 cm). The ratios of total energy, $E_u/E_{p,\eta}$, are 0.91 (h = 563 cm), 0.7 (h = 176 cm), and 1.08 (h = 111 cm), where E is summed over the frequency range 0.05–0.3 Hz. These correspond to H_s errors of 6, 17, and 4%. The larger error just outside the visually observed average breakpoint may be due to the very peaky shape of these waves just prior to breaking.

Figure 5 shows the ratio between the significant wave height using linear theory on the measured velocity (H_s^u) and that obtained from either depth-compensated pressure (H_s^P) or directly measured elevation (H_s^η). Each data point represents a 34-min data run, with variances summed between 0.05 and 0.3 Hz. Sensor pairs not near the breakpoint usually show a discrepancy less than 10% both inside and outside the surf zone. Pairs near the breakpoint have as much as 20% disparity. In both cases, sea surface elevation measurements overpredict the size of the observed velocity fluctuations. The comparisons on a frequency band by frequency band basis are always about as accurate as the total variance comparisons, as in Figure 4. The data shown here are from eight different days with rather different incident wave conditions, varying from narrow banded (November 20, Figure 3) to very broad banded (November 11, Figure 9). Figure 6 illustrates the range of significant wave heights included in Figure 5 and shows that the agreement is good for both small and large waves. It is apparent from Figures 2, 4, 5, and 6 that a single measurement of P, u, or η is sufficient to predict the spectra of the others in the wind wave frequency band with an error of about 20% in both total variance and spectral energy density.

The good agreement between η and u, using linear theory across all frequency bands, suggests that local nonlinearity is not extremely strong. The lowest-order long-wave relationships

$$u = gk\eta/\sigma \qquad p = \rho g\eta \qquad \sigma^2 = ghk^2$$

are approximately valid. The local wave field can be viewed as the superposition of phase-coupled free waves.

SHOALING

The preceding comparisons between pressure, velocity, and sea surface elevations showed that linear theory adequately relates spectra of these quantities to each other at the same horizontal location. Here linear shoaling theory is used to predict spectra in the shoaling regime, given an input spectrum measured in 10-m depth.

Offshore depth profiles used here were taken on November 18, 1978, using shore-based transponders and a portable miniranger for horizontal location and a fathometer for depth. Beach surveys were obtained by rod and transit.

Offshore surveys were taken out to the 15-m contour (x

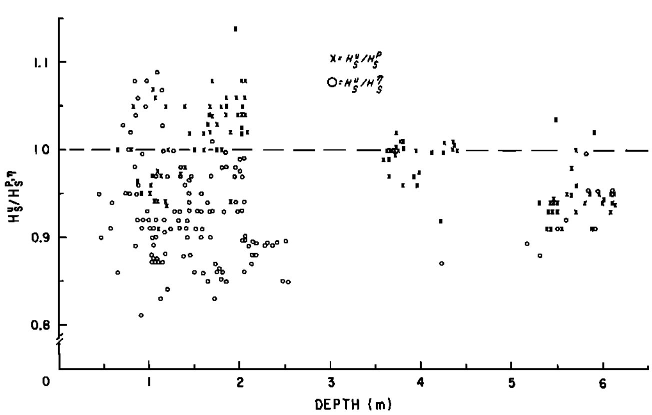

Fig. 5. Ratio of significant wave height inferred from velocity measurements (H_s^u) to that obtained from pressure (H_s^P) or direct sea surface measurements (H_s^η) at various water depths. Values less than 0.9 at 2-m depth are from a single sensor pair, suggesting calibration error.

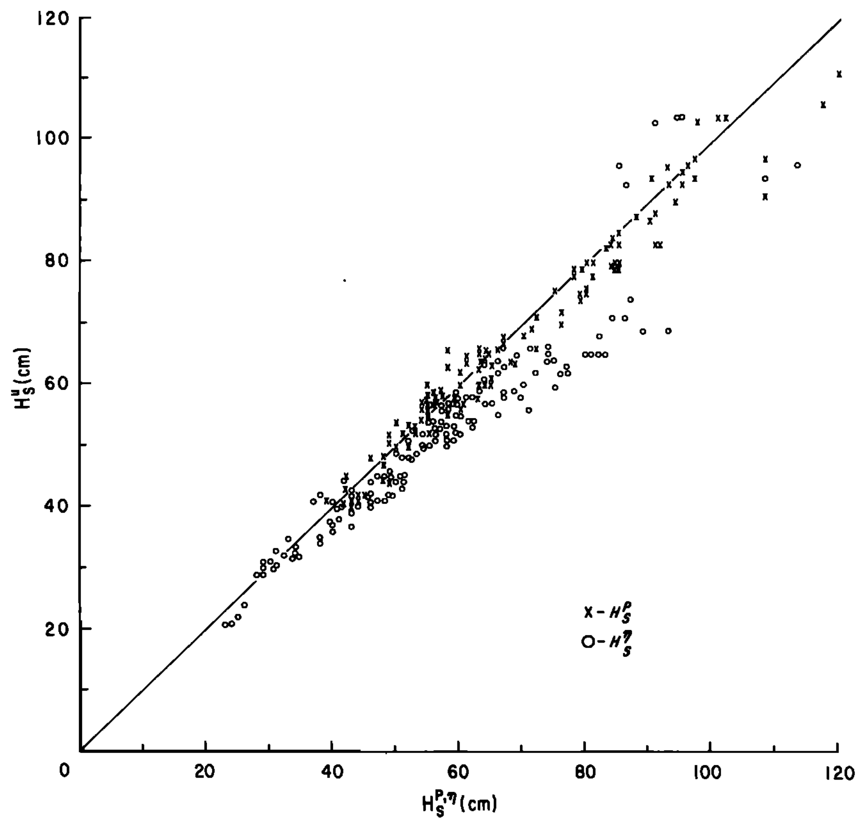

Fig. 6. H_s^u versus H_s^η. The 45° line indicates proper prediction of P, u, η relationships by linear theory.

coordinate) lines, spaced every 40 m in the longshore (y) direction, between $y = -200$ and $y = 0$ m (the onshore-offshore line containing the shoaling wave sensors). Additional depth profiles were obtained at $y = +20$, $+60$, $+160$, and $+320$ m. Surveys were conducted and processed by R. J. Seymour. The topography is essentially featureless, having an approximately constant slope of about 1.3°. Figure 1 shows four representative onshore-offshore profiles and suggests that the contour lines are reasonably parallel, especially in light of the fact that the mean depths obtained from fathometer recordings had the surface waves removed by 'eyeball averaging.'

Figure 1 qualitatively suggests that linear waves propagating over this topography will not behave substantially differently than waves propagating over parallel contours. This speculation was verified by setting up a topographic grid using all survey lines and running a version of *Dobson*'s [1967] linear refraction program. As a test case, waves of 0.067 Hz (corresponding to a typical swell peak in the data) and varying angles of incidence in 10-m depth were refracted from 10- to 3-m depth on the sensor range line. The resulting amplifications of wave heights are compared (Figure 7) with theoretical values calculated by assuming parallel contours and normal incidence.

Figure 7 also shows that on plane-parallel contours, 0.067-Hz waves with a 15° (or less) angle of incidence in 10 m show an amplification in 3 m less than 1.2% different from normally incident waves. If the measured contours were perfectly plane-parallel, the solid and dashed curves in Figure 7 would overlap. Thus waves from the northern quadrant (positive angles) traverse essentially parallel contours, while those from the south exhibit a weak convergence. Waves in 10-m depth at Torrey Pines Beach usually do not have significant energy at angles larger than 15° because refraction further offshore and sheltering by offshore islands significantly reduce energy at larger angles [*Pawka et al.*, 1976]. Within this 15° angular spread the deviation of shoaled wave height amplification over the measured topography compared to normally incident on parallel contours is less than 5% for any directional band. The deviation will be considerably smaller for smooth directional distributions and higher frequencies. Therefore in the following comparisons of energy spectra the effects of directional distributions of energy are neglected, all waves being assumed to impinge normally onto parallel contours. Of course, on a more complex topography it would be necessary to measure the directional spectrum offshore and individually refract each frequency-directional component to the desired location and integrate across all directions to calculate the shoaled energy spectrum. Clearly, the extreme simplicity of the Torrey Pines Beach topography makes the test of linear shoaling much easier than on most beaches.

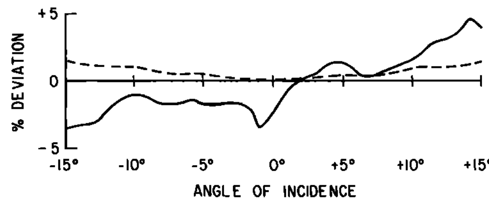

Fig. 7. Percent deviation of wave height amplification of 0.067-Hz waves and varying angles of incidence, shoaled from 10- to 3-m depth over real topography (solid curve) and plane-parallel contours (dashed curve), from the amplification of normally incident waves on plane-parallel contours.

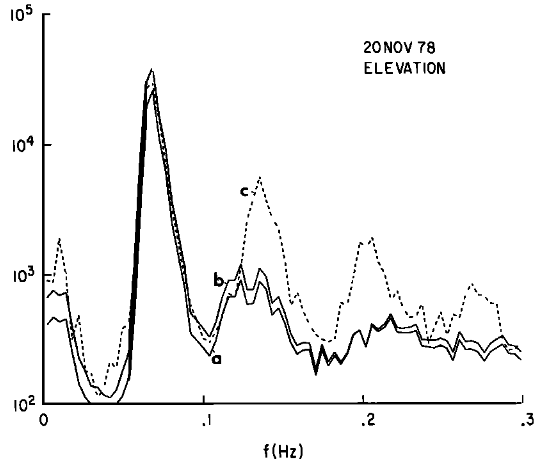

Fig. 8. Elevation spectra (*a*) measured in 1019-cm total depth, P4; (*b*) predicted at $h = 395$ cm; and (*c*) observed at $h = 395$ cm, P16, 32 degrees of freedom.

Measurements were compared with the predictions of linear shoaling theory by using the most seaward pressure sensor (in about 10-m depth) to predict the spectra at shoreward locations. On several occasions, P4 (Figure 1) did not function, so another pressure sensor on the same depth contour, but displaced 66 m in the longshore direction, was used. This had little effect on the results, reconfirming the homogeneity (in a crude sense) of the waves in the longshore direction.

Typical comparisons of observed and predicted spectra (using surface-corrected pressure sensors) are shown in Figures 8 and 9. Figure 8 is typical of narrow-banded (in frequency) incident spectra, and Figure 9 of broad-banded cases. Harmonic amplification due to nonlinearities is evident in Figure 8. The linearly predicted spectrum underestimates the energy at harmonic frequencies and overestimates the energy at the primary frequency. The errors cancel out to some extent, however, so that the total variance is better predicted than the energy content in a particular frequency band (Table 3).

This is in contrast to the previously discussed comparisons of locally measured P, u, and η, where the amount of disagreement is essentially constant with frequency (Figure 4). With broad-banded incident waves (Figure 9) the harmonics of the spectral peak are submerged among energetic high-frequency incident waves, and the agreement is reasonably good across the entire range of frequencies. The predicted total variance (0.05 Hz $< f < 0.3$ Hz) in Figure 9 is 2% greater than that observed. The ability of linear shoaling theory to predict the total variance is summarized in Figure 10 for a variety of days selected for different total energy levels. Current meters, pressure sensors, and wave staffs were all expressed as equivalent (according to linear theory) sea surface elevation spectra, which results in several points at the same depth on the same day. The data, plotted as H_s, generally agree with linear theory for depths greater than about 3 m. Between 2- and 3-m depth the measured variance decreases, even though the visually observed breakpoint was generally between 1- and 2-m depth. For depths less than 2 m, generally in the surf zone, the data for all days cluster together, suggesting saturation. This point will be explored in a later paper.

TABLE 3. Predicted and Observed Harmonic Variances (Figure 8)

	Harmonic Variance, cm²		
	Predicted	Observed	Error, %
Harmonic			
f	401	331	+21
$2f$	23	93	−75
$3f$	17	49	−65
$4f$	9	22	−59
Total variance	502	563	−7.6

CONCLUSIONS

1. A measurement of the P, u, or η spectrum in shallow water at a single horizontal location allows a reasonably good prediction of spectra of the other variables at that location for wind wave frequencies. Errors in both total variance and energy density in a particular frequency band are less than 20% both inside and outside the surf zone. A substantial portion of this error can be attributed to current meter calibration and other experimental uncertainties.

2. On this particularly simple topography, linear shoaling theory gives a semiquantitative prediction of spectra between 2- and 10-m depth. Although total variances are typically predicted with less than 20% error, harmonic amplification and other nonlinear effects can lead to significant errors in the prediction at particular frequency bands. Nonlinear theories

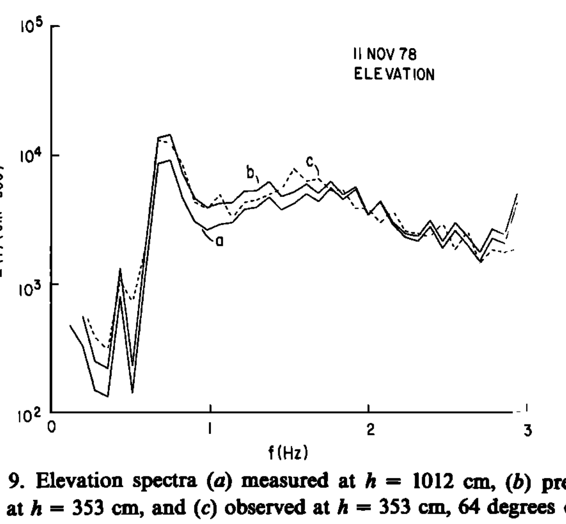

Fig. 9. Elevation spectra (*a*) measured at $h = 1012$ cm, (*b*) predicted at $h = 353$ cm, and (*c*) observed at $h = 353$ cm, 64 degrees of freedom.

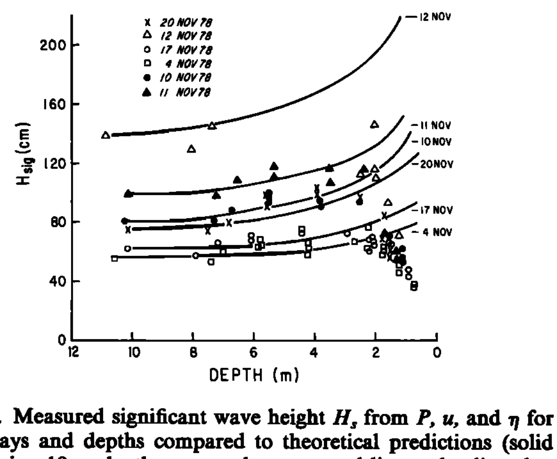

Fig. 10. Measured significant wave height H_s from P, u, and η for various days and depths compared to theoretical predictions (solid curves), using 10-m depth measured spectra and linear shoaling theory.

could undoubtedly improve the agreement on a frequency band by frequency band basis, but it is questionable whether the total variance prediction would be meaningfully improved. The crude treatment of refraction, neglect of wave-current interactions and reflection, and uncertainties regarding the spatial homogeneity of the incident waves on the 10-m contour probably also contribute significant errors.

Acknowledgments. This study was funded by the Office of Naval Research, Geography Branch, under contracts NR 388-114 (E. B. Thornton) and N000014-75-C-0300 (R. T. Guza) and by Sea Grant project R/Cz-N-4D-1. The experiment was one part of a large nearshore dynamics experiment conducted under the Sea Grant National Sediment Transport Study. R. J. Seymour obtained the bathymetric data, and his general assistance and encouragement is gratefully acknowledged. The staff of the Shore Processes Laboratory, SIO, installed and maintained the offshore sensors and data acquisition system. S. S. Pawka did the refraction.

REFERENCES

Bowden, K. F., and R. A. White, Measurements of the orbital velocities of sea waves and their use in determining the directional spectrum, *Geophys. J. Roy. Astron. Soc., 12,* 33–54, 1966.

Bowen, A. J., The generation of longshore currents on a plane beach, *J. Mar. Res., 27,* 206–215, 1969.

Cavaleri, L., J. A. Ewing, and N. D. Smith, Measurement of the pressure and velocity field below surface waves, in *Turbulent Fluxes Through the Sea Surface Wave Dynamics and Predictions, NATO Conf. Ser. V.,* pp. 257–272, Plenum, New York, 1978.

Cunningham, P. M., R. T. Guza, and R. L. Lowe, Dynamics calibration of electromagnetic flow meters, *IEEE Oceans, 79,* 298–301, 1979.

Dobson, R. S., Some applications of a digital computer to hydraulic engineering problems, *Tech. Rep. 80,* Stanford Univ., Stanford, Calif., 1967.

Esteva, D., and D. L. Harris, Analysis of pressure wave records and surface wave records, *Proc. Conf. Coastal Eng. 12th,* 101–116, 1970.

Homma, M., K. Horikawa, and S. Komori, Response characteristics of underwater wave gage, *Proc. Conf. Coastal Eng. 10th,* 99–114, 1966.

Komar, P. D., and D. L. Inman, Longshore sand transport on beaches, *J. Geophys. Res., 75,* 5914–5927, 1970.

Lavelle, J. W., R. A. Yound, D. J. Swift, and T. L. Clarke, Near-bottom sediment concentration and fluid velocity measurements on the inner continental shelf, New York, *J. Geophys. Res., 83,* 6052–6062, 1978.

Longuet-Higgins, M. S., Longshore currents generated by obliquely incident sea waves, 1, *J. Geophys. Res., 75,* 6778–6789, 1970.

Lowe, R. L., D. L. Inman, and B. M. Brush, Simultaneous data system for instrumenting the shelf, *Proc. Conf. Coastal Eng. 13th,* 95–112, 1972.

Madsen, O. S., On the generation of long waves, *J. Geophys. Res., 76,* 8672–8683, 1971.

Mei, C. C., and U. Ünlüata, Harmonic generation in shallow water waves, in *Waves on Beaches and Resulting Sediment Transport,* edited by R. E. Meyer, pp. 181–202, Academic, New York, 1972.

Munk, W. H., and R. S. Arthur, Wave intensity along a refracted ray, *Circ. 521,* pp. 95–108, Nat. Bur. of Stand., Dep. of Commer., Washington, D. C., 1952.

Pawka, S. S., D. L. Inman, R. L. Lowe, and L. Holmes, Wave climate at Torrey Pines Beach, Calif., *Tech. Pap. 76-5,* 372 pp., Coastal Eng. Res. Center, Fort Belvoir, Va., 1976.

Simpson, J. H., Observation of the directional characteristics of waves, *Geophys. J. Roy. Astron. Soc., 17,* 93–120, 1969.

Thornton, E. B., and R. F. Krapohl, Water particle velocities measured under ocean waves, *J. Geophys. Res., 79,* 847–852, 1974.

(Received June 28, 1979;
revised October 29, 1979;
accepted November 6, 1979.)